Article
Vol. 24, No. 5, p. 541–555, October 2020
https://doi.org/10.1007/s12303-019-0039-2
pISSN 1226-4806 eISSN 1598-7477
Geosciences Journal GJ

Source parameters for small-moderate earthquakes in Marmara Region (Turkey)

Tahir Serkan Irmak[1]*, Evrim Yavuz[1], Hamdullah Livaoğlu[1], Erman Şentürk[2], and Emre Y. Sahin[1]

[1]Seismology Section, Department of Geophysics, Kocaeli University, Kocaeli 41100, Turkey
[2]Department of Surveying Engineering, Kocaeli University, Kocaeli 41100, Turkey

ABSTRACT: The main aim of this study is to investigate the self-relation and self-similarity of earthquakes in and around the Marmara Sea (NW Turkey) by using these obtained source parameters. With this purpose, spectral source parameters for 77 small to moderate earthquake ($3.5 \leq M_L \leq 5.2$) that occurred during 2004–2018 have been determined from P and S wave spectra according to Brune's source model by using regional broadband seismograms. The average ratio of P/S wave corner frequency is found to be 1.3 that suggesting higher corner frequency for P wave. The static stress drops range from 0.1 and 136 MPa with a median value of 9.8 MPa (98 bars). The high stress drops for these events can indicate high frictional strength and low strain-rate of the faults. Similarly, the low values of the stress drop can indicate a general weakness of the faults in the study area. There is no clear dependence between the seismic moment and the static stress drop in the analyzed events but some events which have lower seismic moment value also have lower stress drop. Obtaining results indicated the corner frequency decreases with increasing of the seismic moment. Also, a slight depth dependence of the corner frequency has been observed for the analyzed events. Shallower events have larger corner frequency value than deeper events. Also, a clear depth dependence of the stress drop values has not been observed. However, the depth dependence of the seismic moment is seen more clearly. Our results indicated that the deeper events have larger seismic moment values in the study area. In spite of scattering in small events, a linear relationship between local magnitude (M_L) and moment magnitude (M_W) could be obtained as $M_W = 1.4261(\pm 0.31) + 0.6399(\pm 0.08)M_L$ from P waves spectra and $M_W = 0.0136(\pm 0.21) + 0.9883(\pm 0.05)M_L$ from S wave spectra and calculated M_W values are consistent with waveform inversion (centroid moment tensor – CMT) results. These relationships may be useful for seismic hazard studies in the study area.

Key words: Marmara, source parameters, stress drop, corner frequency, seismic moment

Manuscript received November 30, 2018; Manuscript accepted November 10, 2019

1. INTRODUCTION

Most earthquakes are inaccessible to direct observation, therefore it is not easy to determine the source parameters such as seismic moment, stress drop and source dimension by using field observation. The determination of source parameters is important for understanding the physics of earthquakes. However, due to the small number of large earthquakes, small and moderate earthquakes are important in the studies and understanding of the physics of earthquake source. The relations between the source parameters of small to moderate earthquakes provide important information about the earthquake source. Spectral methods are widely used in determination of source parameters of these earthquakes which cannot be observed directly. There are many studies on this subject in the literature following Brune's (1970, 1971) source model (among others, Chouet et al., 1978; Fletcher, 1980; Frankel, 1981; Zobin and Havskov, 1995; Allen et al., 2004; Prieto et al., 2004; Oye et al., 2005; Franceschina et al., 2006; Allman and Shearer, 2007; Tusa and Gresta, 2008; Kumar et al., 2014). However, a few studies in the Marmara region in Turkey have taken place in the literature (Parolai et al., 2007; Gök et al., 2009; Köseoğlu et al., 2014).

The Marmara Region in NW of Turkey is one of the most active seismic areas in Turkey. The North Anatolian Fault Zone (NAFZ) passed through the region and produced several large earthquakes. Three large earthquakes (M > 7 – 1912 Ganos (M_S = 7.3), 1999 Gölcük-Kocaeli (M_W = 7.4) and Düzce (M_W = 7.2))

*Corresponding author:
Tahir Serkan Irmak
Seismology Section, Department of Geophysics, Kocaeli University, Kocaeli 41100, Turkey
Tel: +90-262-3033118, Fax: +90-262-3033102,
E-mail: irmakts@kocaeli.edu.tr

©The Association of Korean Geoscience Societies and Springer 2020

occurred in the last century in the study area (Irmak, 2000). Despite being one of Turkey's most seismically active regions, the number of studies for the determination of source parameters of small moderate earthquakes is small compared to other similar regions in the Earth. Parolai et al. (2007) studied source parameters of the eastern Marmara Region. They studied 523 aftershocks ($0.5 < M_L < 5.9$) of the 1999 Kocaeli earthquake and determined that the stress drop values were changing between 0.002–40 MPa. Parolai et al. (2007) suggested that the seismic moment range between 1.05e14 and 2.41e14 Nm. Köseoğlu et al. (2014) analyzed 174 events ($2.5 < M_L < 5.5$) that occurred western part of Turkey including Marmara region. Köseoğlu et al. (2014) reported that the seismic moments are in range 1.28e14 to 1.66e14 Nm, stress drops on the fault are in range 0.17 to 6476 MPa and corner frequencies are 0.2 to 15 Hz, and the source sizes of the events are 0.0862 to 5.1042 km. The different scaling relation between stress drop and event magnitudes for similar size earthquakes has been observed in the study of Parolai et al. (2007) and Köseoğlu et al. (2014).

In this study, we tried to determine the source parameters of small to moderate earthquakes occurring in the Marmara region by using the P and S wave spectrum and to establish meaningful relationships between these parameters. The seismic moment was used to derive new empirical relationships with the local magnitude M_L. The results can be used to understand the source properties of the earthquakes occurring in the region as well as in seismic hazard studies.

2. SEISMOTECTONIC OF THE REGION

NW Turkey contains a number of tectonically active basins that formed by right-lateral strike-slip NAFZ (Fig. 1). The NAFZ is one of the largest strike-slip faults in the world and is known for its similarity to the San Andreas Fault in California. The NAFZ is running east to west from Karliova (41.0°E) to Bolu (31.5°E) as a relatively simple, narrow, right-lateral strike-slip fault zone. It is divided into two branches in the Marmara region so that the deformation becomes distributed over a 120 km wide zone and when it enters the Aegean Sea, it has a more diffuse structure than its appearance in the east (Sato et al., 2004). The annual rate of the NAFZ is around 20–30 mm/year and is separating the Anatolia-Eurasian plates (e.g., Ambraseys, 1970; Toksöz et al., 1979; Barka and Kadinsky-Cade, 1988; Taymaz et al., 1991; Barka, 1992; Smith et al., 1995; Stein et al., 1997; Nalbant et al., 1998; Armijo et al., 1999, 2000; Barka, 1999; Hubert-Ferrari et al., 2000; McClusky et al., 2000; Okay et al., 2000; Reilinger et al., 2000; Imren et al., 2001; Le Pichon et al., 2001; Irmak et al., 2007; Tunç et al., 2011; Kinscher et al., 2013). The NAFZ has produced number of large earthquakes (M > 7) and ruptured over most of its length during

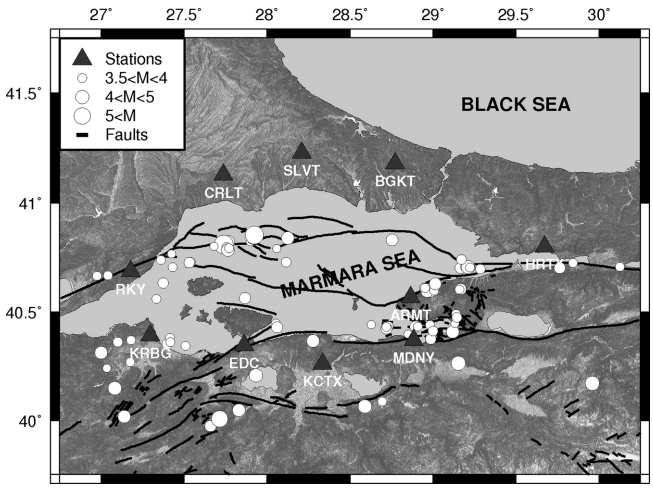


Fig. 1. Map of the study area, red circles represent studied earthquakes according to their size, while blue triangles represent stations. Black lines indicate main branches of the North Anatolian Fault Zone.

the last century between 1939 and 1999 (Ambraseys, 1970; Barka, 1996; Stein et al., 1997). The last two earthquakes in the Marmara region were the 1912 Mürefte earthquake occurring in the west of the region and the 1999 earthquake that occurred in the east of the region. The area between the two earthquake rupture, which comes to the central part of the Marmara region, has remained silent since the earthquake of 1766 (Stein et al., 1997; Bulut et al., 2009).

The Marmara region, especially the Marmara Sea, exhibits a complex tectonic structure. Several studies have been carried out to infer tectonic models for the Marmara Sea region after the devastating 1999 Kocaeli earthquake ($M_W = 7.4$), but the fault structure below the Marmara Sea is still complex and debated. There are two different views on the region. The first is described by Le Pichon et al. (2001). They have defined a single localized through-going right-lateral strike-slip fault segment in the region. The second is described by Armijo et al. (2002). They reinterpreted it as a composition of several oblique extensional segments, separated by zones of distributed deformation (Sato et al., 2004). On the other hand, this region is defined as a transition zone from NAFZ's strike-slip regime to the extensional regime in the Aegean Sea by Sato et al. (2004). However, the common idea or acceptance is that of the NAFZ below the Marmara Sea consists of three pull-apart sub- basins (Armijo et al., 1999, 2002, 2005; Imren et al., 2001; Le Pichon et al., 2001, 2003; Demirbag et al., 2003; Karabulut et al., 2003; Kurtulus and Canbay, 2007; Bayrakci et al., 2013; Fichtner et al., 2013a, 2013b).

3. DATA AND METHODOLOGY

The waveform data which belongs to 77 earthquakes in the magnitude range 3.5–5.2 used in this study were selected from

the broadband seismic stations of the Kandilli Observatory and Earthquake Research Institute (KOERI) with the sampling rate of 100 sps during 2004 to 2018. The stations and earthquake epicenters which have used are shown in Figure 1.

P (vertical component) and S wave (transverse component) amplitude spectra have been used for the spectral analysis. We used at least three stations records which were recorded at different distances for each event. For P wave analysis, 1.5 sec time window which is dependent on the earthquake magnitude has been selected for all analyzed events. The all seismograms belongs to analyzed events have been tapered by a Haning window. All seismograms have been recorded by velocity seismographs. First, baseline correction has been done by removing the mean. Then instrument response has been deconvolved and finally, all seismograms convert to displacement. The Brune's ω^{-2} model has been used for fitting the observed P wave spectra (Fig. 2). For S wave, window length was chosen as 10–30 s, depending on the magnitude and distance to the source.

The observed displacement amplitude spectrum is described as follows;

$$U(f \cdot R) = G(R) \cdot S(f) \cdot A(f \cdot t), \quad (1)$$

where f is the frequency, R is the hypocentral distance, $G(R)$ the attenuation generated by geometrical spreading, $S(f)$ the amplitude source spectrum, $A(f.t)$ the anelastic attenuation, t the travel time. To eliminate the negative effects of attenuation and geometrical spreading on amplitudes, the observed displacement spectrum ($U(f{\cdot}R)$) has been corrected for attenuation and geometrical spreading. Then, the source spectrum (S(f)) has been determined.

All analyzed earthquakes were within 100 km distance, therefore following Havskov and Ottomöller (2010) $G(R) = 1/R$ was assumed for P and S waves as the attenuation due to geometrical spreading. For attenuation correction, a frequency-

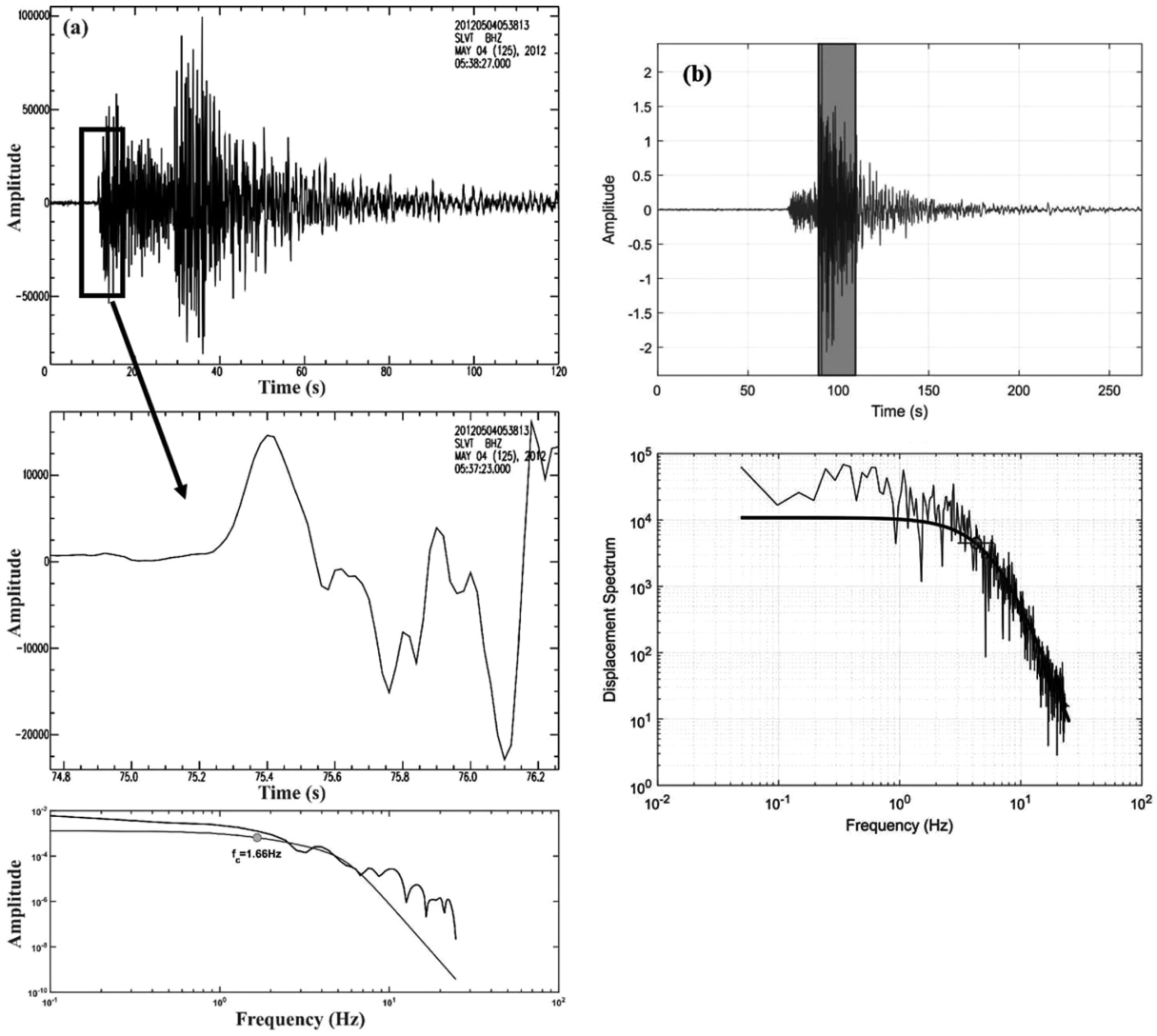


Fig. 2. Waveform example of (a) P and (b) S waves. Lower part of the figure shows spectra and determined corner frequency (f_c).

https://doi.org/10.1007/s12303-019-0039-2

dependent attenuation relation (Horasan et al., 1998)

$$Q_S = (50 \pm 1.7)f^{1.09\pm0.05}, \quad (2)$$

and $Q_p \geq 2Q_s$ have been applied.

Then, spectral source parameters, corner frequency (f_c), source radius (r), seismic moment (M_o), stress drop ($\Delta\sigma$), and moment magnitude (M_W) were estimated by using corrected source spectrum. Kumar et al. (2012) algorithm was used to estimate the source parameters.

The seismic moment has been calculated using the value of Ω_o and the following equation (Keilis-Borok, 1960; Haskell, 1964; Brune, 1970, 1971):

$$M_0(V_{P,S}) = 4 \cdot \pi\rho \cdot RV_{P,S}^3 \cdot \frac{\Omega_o(P,S)}{k \cdot R_{\theta\phi}(P,S)}, \quad (3)$$

where ρ is the average density ($\rho = 2.67$ g/cm^3), $V_{P,S}$ is P and S wave velocity in earthquake source zone, respectively. R is the hypocentral distance that causes geometrical spreading. Ω_o is low frequency spectral level. $R_{\theta\phi}$ is the average radiation pattern ($R_{\theta\phi} = 0.52$ for P wave and $R_{\theta\phi} = 0.63$ for S wave), and k is free surface amplification ($k = 2$), (Boatwright, 1980). Kalafat et al. (1987) velocity model was used both for source area and beneath receiver structure.

The moment magnitude has been calculated the following equation proposed by Hanks and Kanamori (1979):

$$Mw = \left(\frac{2}{3} * \log_{10}(M_o)\right) - 10.7. \quad (4)$$

The source radius and the stress drop have been calculated following equation (Hanks and Wyss. 1972):

$$r = \frac{2.34\,V_p}{2\pi f_0}, \quad (5)$$

$$\Delta\sigma = \frac{7}{16} \cdot \frac{M_0}{r^3}. \quad (6)$$

4. RESULTS AND DISCUSSION

The results obtained using displacement spectra of P and S waves are given in Tables 1 and 2, respectively. The determined

Table 1. Obtained spectral source parameters for P waves of the analyzed events

	Date	h (km)	M_L	$f_{c(P)}$ (Hz)	M_w	$M_{o(S)}$	r_P (m)	$\Delta\sigma_{(P)}$ (MPa)	Number of Used Stations
1	20071209_032009	15	3.6	7.1	3.6 ± 0.4	2.84E + 14	313.4	4.0	4
2	20080412_032520	10.1	3.6	2.1	4.2 ± 0.5	1.90E + 15	1090.0	0.6	5
3	20080629_082801	6.8	3.7	4.8	3.8 ± 0.3	5.40E + 14	466.5	2.3	4
4	20080709_045448	6.4	3.6	10.7	3.9 ± 0.4	6.70E + 14	209.8	31.7	6
5	20080710_074953	13.6	4.9	2.1	4.6 ± 0.4	7.60E + 15	1090.0	2.6	6
6	20080714_160212	7.9	3.7	8.3	3.8 ± 0.3	6.30E + 14	269.2	14.1	8
7	20081005_060405	15.3	4.1	7.1	4.3 ± 0.2	3.24E + 15	313.4	46.1	10
8	20081022_010035	8.3	3.6	4.0	4.0 ± 0.2	1.15E + 15	557.3	2.9	4
9	20090123_163450	14.9	3.5	3.6	3.9 ± 0.4	8.42E + 14	617.3	1.6	4
10	20090124_155838	16.5	4.2	2.1	4.4 ± 0.3	5.25E + 15	1090.0	1.8	10
11	20090125_032652	14.5	3.6	3.2	4.0 ± 0.3	9.46E + 14	691.8	1.3	10
12	20090318_163337	10.9	3.7	3.2	3.9 ± 0.2	8.36E + 14	691.8	1.1	7
13	20090427_190306	18.3	4.1	1.7	4.7 ± 0.5	1.34E + 16	1346.1	2.4	5
14	20090523_215700	10.8	3.8	13	3.8 ± 0.4	6.19E + 14	172.0	53.2	6
15	20090622_092911	5.8	3.6	6.4	3.8 ± 0.4	4.77E + 14	351.9	4.8	7
16	20090718_095952	6.7	3.6	6.4	3.8 ± 0.4	5.66E + 14	351.9	5.7	7
17	20090801_164238	10.0	4.1	4.8	4.1 ± 0.3	1.83E + 15	466.5	7.9	7
18	20091116_184722	13.7	3.7	5.6	3.7 ± 0.4	3.68E + 14	401.2	2.5	9
19	20100203_215755	9	3.5	14.9	3.7 ± 0.5	4.55E + 14	149.6	59.5	3
20	20100308_160711	2.8	3.5	4.8	3.5 ± 0.5	2.21E + 14	466.5	1.0	5
21	20100313_011921	16	3.6	4.0	4.0 ± 0.6	9.43E + 14	557.3	2.4	9
22	20101003_174903	11.8	4.4	1.7	4.6 ± 0.4	8.30E + 15	1346.1	1.5	5
23	20101026_220940	10.2	3.5	9.5	3.5 ± 0.3	1.68E + 14	235.7	5.7	7
24	20110120_020937	11.7	4.3	15.3	3.8 ± 0.8	5.43E + 14	145.8	76.7	7
25	20110225_092009	6.9	3.9	9.8	4.1 ± 0.4	1.60E + 15	226.4	60.3	6
26	20110309_070403	9.4	4	2.1	4.0 ± 0.7	1.16E + 15	1090.0	0.4	8
27	20110309_070612	3.0	3.7	3.2	3.7 ± 0.6	8.32E + 14	691.8	1.1	5
28	20110330_170720	7.9	4.4	4.4	4.1 ± 0.5	1.36E + 15	507.9	4.5	7

Table 1. (continued)

	Date	h (km)	M_L	$f_{c(P)}$ (Hz)	M_w	$M_{o(S)}$	r_P (m)	$\Delta\sigma_{(P)}$ (MPa)	Number of Used Stations
29	20110530_084230	13.1	3.6	4.0	3.5 ± 0.8	1.75E + 14	557.3	0.4	7
30	20110711_160912	6.5	4.7	2.1	4.4 ± 0.4	3.77E + 15	1090.0	1.3	7
31	20110725_175720	17.0	5.2	2.8	4.5 ± 0.4	6.69E + 15	789.6	6.0	4
32	20110725_204352	7.2	3.5	2.8	3.7 ± 0.4	3.45E + 14	789.6	0.3	8
33	20110804_083519	2.0	3.5	8.3	3.7 ± 0.8	3.59E + 14	269.2	8.1	8
34	20110811_133711	4.8	3.6	10.7	3.8 ± 0.2	5.15E + 14	209.8	24.4	5
35	20110816_173006	5.4	4	11.4	4.0 ± 0.3	9.49E + 14	195.5	55.6	8
36	20111016_034225	7.0	3.8	6.7	3.7 ± 0.6	3.59E + 14	331.5	4.3	5
37	20120112_185231	7.1	3.6	4.4	3.4 ± 0.3	1.32E + 14	507.9	0.4	7
38	20120504_053813	12.0	4.3	3.2	4.1 ± 0.6	1.66E + 15	691.8	2.2	8
39	20120607_205425	14.9	5.1	0.9	4.9 ± 0.8	2.21E + 16	2539.3	0.6	9
40	20120808_130229	5.9	3.5	8.7	3.2 ± 0.1	8.29E + 13	257.1	2.1	5
41	20121026_033736	8.3	4	12.2	3.7 ± 0.2	3.70E + 14	183.0	26.4	7
42	20121027_023759	6.3	3.7	12.6	3.6 ± 0.3	2.94E + 14	177.3	23.1	7
43	20130817_181630	5.5	4.1	4.0	3.9 ± 0.3	8.80E + 14	557.3	2.2	6
44	20130925_133944	7.5	3.6	7.9	3.5 ± 0.4	2.13E + 14	282.5	4.1	7
45	20131003_102607	13.8	3.7	3.2	3.8 ± 0.5	6.65E + 14	691.8	0.9	8
46	20131127_041337	10.8	4.7	1.7	4.5 ± 0.8	5.89E + 15	1346.1	1.1	8
47	20140511_050700	11.0	3.6	6.4	3.6 ± 0.6	2.57E + 14	351.9	2.6	9
48	20140601_211745	11.0	3.6	7.1	3.8 ± 0.3	6.29E + 14	313.4	8.9	8
49	20140703_050446	11.8	4.6	2.8	4.8 ± 0.4	1.96E + 16	789.6	17.4	8
50	20140803_104244	3.4	3.6	7.1	3.9 ± 0.3	7.39E + 14	313.4	10.5	7
51	20140803_222244	11.5	4	5.6	4.1 ± 0.6	1.45E + 15	401.2	9.8	6
52	20141216_090213	12.9	4.4	1.7	4.5 ± 0.9	6.93E + 15	1346.1	1.2	6
53	20150123_101942	5.0	4.5	4.4	4.2 ± 0.3	1.91E + 15	507.9	6.4	6
54	20150511_041627	8.1	3.9	5.6	3.9 ± 0.4	7.09E + 14	401.2	4.8	4
55	20150813_010128	9.4	3.8	7.5	3.7 ± 0.2	3.94E + 14	297.2	6.6	5
56	20150829_124752	10.1	3.6	8.7	3.6 ± 0.6	2.98E + 14	257.1	7.7	7
57	20151028_162002	14.3	4.5	2.4	4.5 ± 0.4	7.35E + 15	915.8	4.2	10
58	20151105_122936	13.5	3.7	4.0	3.8 ± 0.8	5.82E + 14	557.3	1.5	9
59	20151116_154543	12.6	4.2	6.0	3.9 ± 0.4	7.54E + 14	374.9	6.3	9
60	20151207_205751	10.3	3.7	9.1	3.6 ± 0.3	2.84E + 14	246.1	8.3	7
61	20160130_090314	9.8	3.5	4.8	3.6 ± 0.3	2.43E + 14	466.5	1.1	6
62	20160327_050354	14.7	3.7	7.1	3.4 ± 1.2	1.37E + 14	313.4	2.0	6
63	20160328_172346	15.5	3.7	7.9	3.2 ± 0.5	6.85E + 13	282.5	1.3	6
64	20160607_040945	15.8	4.6	3.2	4.4 ± 0.2	4.55E + 15	691.8	6.0	6
65	20160607_080215	13.5	3.5	7.1	3.4 ± 0.3	1.38E + 14	313.4	2.0	5
66	20160622_233559	7.6	3.6	4.4	3.2 ± 0.3	6.39E + 13	507.9	0.2	5
67	20160625_054011	9.3	4.4	3.6	3.8 ± 0.2	6.35E + 14	617.3	1.2	7
68	20160709_142051	9.5	3.6	1.3	4.1 ± 0.7	1.48E + 15	1759.5	0.1	4
69	20160717_085541	11.4	4	2.8	4.0 ± 0.3	1.01E + 15	789.6	0.9	5
70	20160902_192457	9.0	3.7	9.1	4.0 ± 0.5	1.06E + 15	278.2	28.5	4
71	20161008_230246	5.5	3.7	11.0	4.1 ± 0.2	1.38E + 15	549.4	27.3	6
72	20170420_141121	6.4	4.3	2.8	3.4 ± 0.3	1.45E + 14	1072	0.3	7
73	20170722_221231	13.2	4.3	6.0	3.1 ± 0.3	4.83E + 13	326.5	0.7	5
74	20170725_152110	7.2	3.6	6.4	4.3 ± 0.2	2.70E + 15	308.6	92.5	6
75	20171231_201202	12.6	4.1	6.4	4.3 ± 0.1	3.52E + 15	608.8	121.4	8
76	20181130_023635	12.1	4.3	5.2	5.0 ± 0.2	4.21E + 16	4486.1	110	9
77	20181204_123803	11.3	3.6	2.4	4.4 ± 0.3	4.30E + 15	459.7	2.7	6

https://doi.org/10.1007/s12303-019-0039-2

Table 2. Obtained spectral source parameters for S waves of the analyzed events

	Date	h (km)	M_L	f_{cS} (Hz)	M_w	$M_{o(S)}$	r_S (m)	$\Delta\sigma_{(S)}$ (MPa)	Number of Used Stations
1	20071209_032009	15	3.6	4.7	3.4 ± 0.2	1.29E +14	271.8	3.3	4
2	20080412_032520	10.1	3.6	1.64	3.7 ± 0.5	1.03E + 15	1002.0	0.4	5
3	20080629_082801	6.8	3.8	4.30	3.6 ± 0.2	3.40E + 14	304.1	2.3	4
4	20080709_045448	6.4	3.6	5.1	3.4 ± 0.3	4.35E + 15	260.5	6.5	6
5	20080710_074953	13.6	4.9	1.7	4.7 ± 0.3	1.73E + 16	863.5	13.5	6
6	20080714_160212	7.9	3.7	7.0	3.5 ± 0.4	4.53E + 14	351.4	15.2	8
7	20081005_060405	15.3	4.2	3.2	4.1 ± 0.1	1.83E + 15	547.9	17.6	10
8	20081022_010035	8.3	3.8	3.9	3.8 ± 0.2	6.58E + 14	450.4	7.1	4
9	20090123_163450	14.9	3.7	5.6	3.6 ± 0.2	3.12E + 14	381.1	11.8	4
10	20090124_155838	16.5	4.1	5.3	4.1 ± 0.3	2.44E + 15	551.2	54.0	10
11	20090125_032652	14.5	3.5	6.4	3.5 ± 0.2	2.09E + 14	245.5	13.2	10
12	20090318_163337	10.9	3.7	3.6	3.7 ± 0.2	5.77E + 14	426.1	5.1	7
13	20090427_190306	18.3	3.9	4.9	4.2 ± 0.1	1.93E + 15	300.6	59.5	5
14	20090523_215700	10.8	3.8	3.0	3.9 ± 0.1	9.92E + 14	538.1	9.8	6
15	20090622_092911	5.8	3.7	3.4	3.8 ± 0.2	6.36E + 14	557.8	13.2	7
16	20090718_095952	6.7	3.6	4.6	3.7 ± 0.2	4.74E + 14	376.8	11.0	7
17	20090801_164238	10.0	4.3	4.7	3.9 ± 0.2	8.84E + 14	330.4	36.3	7
18	20091116_184722	13.7	3.6	6.3	3.2 ± 0.1	8.83E + 13	213.4	4.8	9
19	20100203_215755	9	3.5	8.3	3.6 ± 0.4	4.85E + 14	249.0	54.5	3
20	20100308_160711	2.8	3.5	5.6	3.6 ± 0.3	5.10E + 14	242.6	30.1	5
21	20100313_011921	16	3.6	8.0	3.4 ± 0.2	2.06E + 14	187.5	22.2	9
22	20101003_174903	11.8	4.3	3.8	4.2 ± 0.2	3.24E + 15	643.8	83.1	5
23	20101026_220940	10.2	3.5	6.3	3.4 ± 0.2	1.74E + 14	287.7	12.1	7
24	20110120_020937	11.7	4.1	5.5	3.9 ± 0.3	1.54E + 15	242.5	52.7	7
25	20110225_092009	6.9	3.8	7.8	3.5 ± 0.1	2.37E + 14	188.5	40.3	6
26	20110309_070403	9.4	4	4.7	3.9 ± 0.4	2.08E + 15	659.0	30.9	8
27	20110309_070612	3.0	3.7	4.8	3.6 ± 0.3	4.42E + 14	582.6	7.8	5
28	20110330_170720	7.9	4.3	3.7	4.2 ± 0.5	7.83E + 15	769.2	22.4	7
29	20110530_084230	13.1	3.6	6.0	3.3 ± 0.2	1.27E + 14	240.3	10.1	7
30	20110711_160912	6.5	4.6	3.4	4.2 ± 0.2	3.30E + 15	589.8	42.7	7
31	20110725_175720	17.0	5.2	1.55	5.0 ± 0.1	3.85E + 16	842.3	27.4	4
32	20110725_204352	7.2	3.5	2.5	3.7 ± 0.3	7.15E + 14	776.5	2.1	8
33	20110804_083519	2.0	3.5	5.3	3.5 ± 0.5	8.98E + 14	526.7	6.6	8
34	20110811_133711	4.8	3.6	9.5	3.7 ± 0.3	5.92E + 14	158.0	161.7	5
35	20110816_173006	5.4	4	4.0	4.0 ± 0.4	2.21E + 15	614.2	51.1	8
36	20111016_034225	7.0	3.8	6.4	3.6 ± 0.2	3.16E + 14	213.6	18.6	5
37	20120112_185231	7.1	3.5	6.6	3.5 ± 0.4	4.37E + 14	401.1	10.4	7
38	20120504_053813	12.0	4.3	2.6	4.2 ± 0.3	2.58E + 15	800.5	8.5	8
39	20120607_205425	14.9	5.1	0.6	5.3 ± 0.3	1.68E + 17	3875.9	6.0	9
40	20120808_130229	5.9	3.5	6.8	3.3 ± 0.2	1.29E + 14	205.2	13.8	5
41	20121026_033736	8.3	4	6.3	3.6 ± 0.2	3.99E + 14	298.4	34.5	7
42	20121027_023759	6.3	3.9	2.3	3.9 ± 0.3	1.13E + 14	1170.1	7.3	7
43	20130817_181630	5.5	4.2	3.3	4.2 ± 0.3	3.90E + 14	534.4	73.9	6
44	20130925_133944	7.5	3.5	8.0	3.2 ± 0.1	6.93E + 13	185.6	15.1	7
45	20131003_102607	13.8	3.7	4.0	3.7 ± 0.2	6.95E + 14	895.2	9.2	8
46	20131127_041337	10.8	4.8	1.8	5.0 ± 0.5	7.27E + 16	2067.4	1.06	8
47	20140511_050700	11.0	3.6	9.0	3.4 ± 0.3	2.43E + 14	157.2	35.9	9
48	20140601_211745	11.0	3.6	9.5	3.6 ± 0.3	3.40E + 14	183.8	57.5	8
49	20140703_050446	11.8	4.5	2.4	4.8 ± 0.5	2.22E + 16	910.0	39.0	8
50	20140803_104244	3.4	3.6	5.2	3.7 ± 0.3	5.75E + 14	894.2	26.2	7

Table 2. (continued)

	Date	h (km)	M_L	f_{cS} (Hz)	M_w	$M_{o(S)}$	r_S (m)	$\Delta\sigma_{(S)}$ (MPa)	Number of Used Stations
51	20140803_222244	11.5	4.1	1.95	4.2 ± 0.4	4.36E + 15	881.1	4.3	6
52	20141216_090213	12.9	4.4	3.7	4.3 ± 0.3	4.29E + 15	902.2	39.2	6
53	20150123_101942	5.0	4.5	1.5	4.7 ± 0.4	1.71E + 16	1098.7	14.3	6
54	20150511_041627	8.1	3.9	4.1	3.9 ± 0.2	9.18E + 14	366.6	12.2	4
55	20150813_010128	9.4	3.8	6.1	3.7 ± 0.3	5.32E + 14	234.3	24.4	5
56	20150829_124752	10.1	3.6	6.3	3.5 ± 0.2	2.16E + 14	233.3	18.7	7
57	20151028_162002	14.3	4.5	2.3	4.6 ± 0.3	1.32E + 16	762.4	43.3	10
58	20151105_122936	13.5	3.8	5.3	3.9 ± 0.3	1.37E + 15	772.4	45.9	9
59	20151116_154543	12.6	4.2	4.0	4.2 ± 0.3	3.38E + 14	557.6	29.3	9
60	20151207_205751	10.3	3.7	5.3	3.7 ± 0.4	7.15E + 14	329.7	25.0	7
61	20160130_090314	9.8	3.5	5.4	3.6 ± 0.2	3.60E + 14	349.5	13.8	6
62	20160327_050354	14.7	3.7	6.5	3.6 ± 0.3	4.60E + 14	255.9	31.8	6
63	20160328_172346	15.5	3.7	8.3	3.5 ± 0.3	3.22E + 14	163.0	49.1	6
64	20160607_040945	15.8	4.6	5.1	4.5 ± 0.2	7.48E + 15	434.1	485.7	6
65	20160607_080215	13.5	3.5	6.7	3.6 ± 0.1	2.76E + 14	243.4	31.9	5
66	20160622_233559	7.6	3.6	3.2	4.1 ± 0.2	1.51E + 13	603.2	14.7	5
67	20160625_054011	9.3	4.5	2.5	4.5 ± 0.3	8.31E + 15	845.1	22.4	7
68	20160709_142051	9.5	3.6	4.0	3.9 ± 0.5	2.31E + 15	622.4	14.9	4
69	20160717_085541	11.4	4	2.8	4.0 ± 0.4	1.01E + 15	789.6	0.9	5
70	20160902_192457	9.0	3.7	5.7	3.6 ± 0.4	6.46E + 14	369.2	7.7	4
71	20161008_230246	5.5	3.7	5.7	3.8 ± 0.2	8.97E + 14	328.6	38.8	6
72	20170420_141121	6.4	4.3	1.7	4.5 ± 0.5	1.15E + 16	1434.6	8.8	7
73	20170722_221231	13.2	4.3	5.1	4.1 ± 0.3	2.95E + 15	409.9	119.1	5
74	20170725_152110	7.2	3.6	5.1	3.9 ± 0.3	1.10E + 15	320.3	75.9	6
75	20171231_201202	12.6	4.1	4.4	4.2 ± 0.2	3.10E + 15	520.0	136.0	8
76	20181130_023635	12.1	4.3	5.0	4.3 ± 0.2	3.31E + 15	367.5	169.3	9
77	20181204_123803	11.3	3.6	5.9	3.7 ± 0.3	5.61E + 14	278.8	23.8	6

corner frequency (f_c) for all analyzed events is varying from 0.9 to 15.3 *Hz* for P wave and 0.6 to 9.5 for S wave. Figure 3 shows dependence of corner frequency (f_c) and stress drop on seismic moment. Figure 3a indicates that the corner frequency decreases with the increase of the seismic moment. As can be seen in Figure 3a, f_c(P) is larger than f_c(S) and f_c(P)/f_c(S) ratio is 1.3 which is comparable to value of 1.5 was obtained by several researchers (among others, Fletcher, 1980; Boatwright et al., 1991; Abercrombie, 1995; Garcia et al., 2004; Prieto et al., 2004; Süle and Weber, 2013; Ataeva et al., 2015). According to Sivaram et al. (2013), lower f_c(P)/f_c(S) value may be due to nondouble-couple source and/or specific take off angle of observation. They, also concluded that scattering and insufficient sampling rate could be resulted unsuccessful estimation of f_c. Although the f_c(P)/f_c(S) ratio that we found is close to the value in the literature, these may be reason that why f_c(P)/f_c(S) ratio is relatively small.

Seismic moments obtained from P waves (M_o(P)), range from 4.83e13 Nm to 4.21e16 Nm and, from S waves (M_o(S)), 1.51e13 Nm to 1.68e17 Nm. The average ratio is 1.06. Similar values have been obtained for small earthquakes to Hungary as 0.97 by Süle and Weber (2013), to Kumaon, Himalaya as 1.04 by Sivaram et al. (2013), to India as 1.11 by Kumar et al. (2014) among others. The source radii obtained from P waves range from 146 to 4486 m, and from S waves range from 257 to 3876 m. The average ratio is 1.1. This value is also comparable to the studies that have done by several researches (among others, Garcia et al., 2004; Sivaram et al., 2013; Süle and Weber, 2013; Kumar et al., 2014; Ataeva et al., 2015).

Static stress drop value is one of the important source parameters which measures the stress decrease after an earthquake averaged over the fault or rupture surface area. The calculated stress drop values vary from 0.1 to 121 MPa for P wave (with a median of 2.9 MPa) and 0.4 to 136 MPa for S wave (event no 65 which have 486 MPa was ignored in the analysis) (with a median of 17.8 MPa). Considering both P and S waves, median value was calculated to be 9.8 MPa. Such a scattering in stress drop for small events have been reported by several researchers (among others, Jin et al., 2000; Allman and Shearer, 2009; Kumar et al., 2015; Wu and Chapman, 2017). Allman and Shearer (2009) estimates stress drop ranging from 0.3 to 50 MPa independent

https://doi.org/10.1007/s12303-019-0039-2

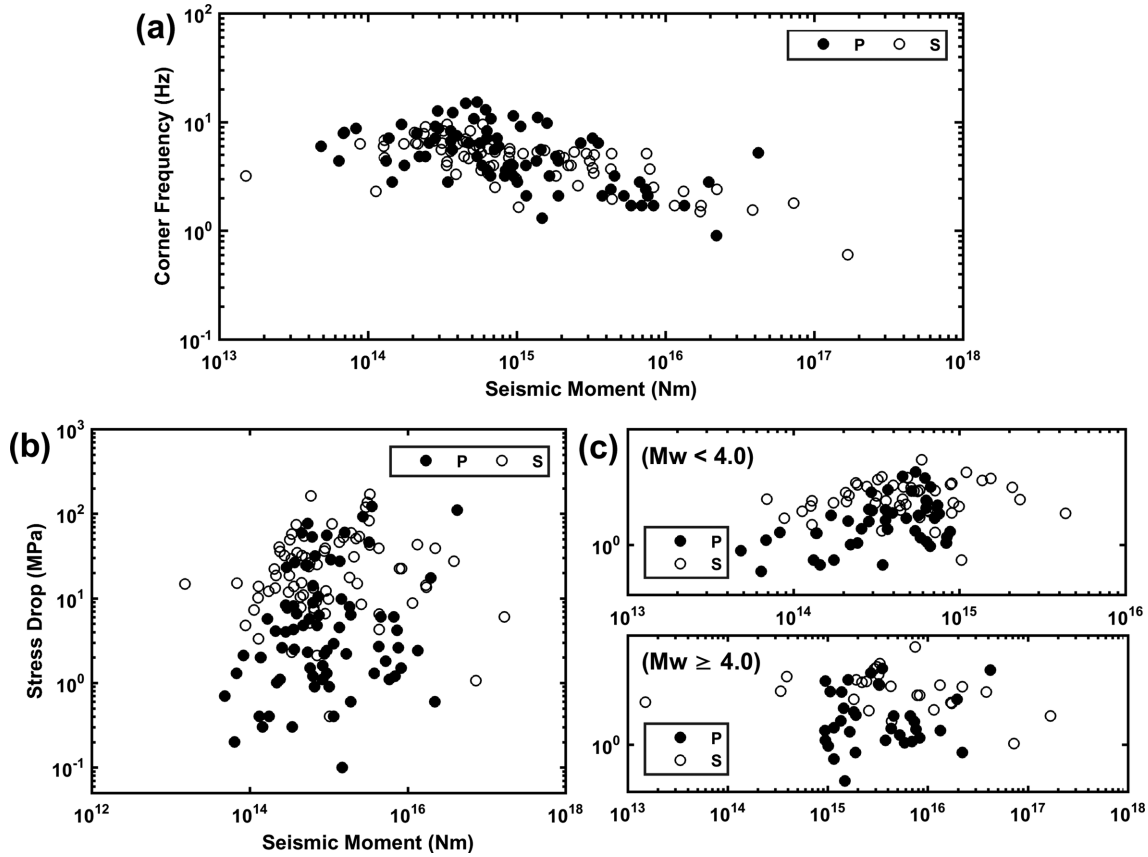


Fig. 3. Relationship between (a) corner frequency and seismic moment and (b) stress drop and seismic moment determined from P (black circles) and S (white circles) wave spectra. (c) The events with the magnitudes smaller than 4 (upper) and larger than 4 (lower).

of moment for global earthquakes from M_W 5.2 to 8.3. Oth et al. (2010) found stress drop ranging from 0.1 to 100 MPa for crustal events ranging from 2.7–8 in Japan. Wu and Chapman (2017) analyzed 2011 Mineral Virginia Earthquake and its aftershocks ($M_W \geq 2.5$) and found that the stress drops are varying between 0.02 and 67 MPa with a median of 3 MPa. Wu and Chapman (2017) indicated that a smaller earthquake can rupture on just high or low stress drop asperity and hence smaller events can have larger variations in stress drop. The seismic moment and the static stress drop relationship is also shown in Figure 3b. Even though there is no clear dependence between the seismic moment and the static stress drop, it can be observed from Figure 3c, there is a turning point around magnitude 4. The stress drop values for the events with the magnitudes smaller than 4 are increasing with the magnitude (Fig. 3c).

Several studies (among others, Jones and Helmberger, 1996; Hardebeck and Hauksson, 1997; Bilek and Lay, 1998; Asano et al., 2003; Allmann and Shearer, 2007, 2009; Hardebeck and Aron, 2009; Candela et al., 2011; Huang et al., 2017; Wu et al., 2018) have found a depth dependence of stress drop. The depth dependence of stress drop in the shallow crust has been explained by Allmann and Sherar (2007) due to S wave variation and Bilek and Lay (1998) due to rigidity variation in a subduction slab. Huang et al. (2017) explained that increase of effective normal stress can cause depth dependence of stress drops. Allmann and Shearer (2007) studied stress drop variations in small earthquakes near Parkfield. California and indicated that they could not resolved any increase of stress drop with depth. Parolai et al. (2007) analyzed 523 aftershocks of 1999 Kocaeli earthquake and resulted that the stress drop value show tendency of increasing with aftershock magnitude. Allmann and Shearer (2007) also concluded that depth dependence of stress drop is very sensitive to the chosen velocity model. Wu and Chapman (2017) studied 2011 Mineral Virginia Earthquake and its aftershocks and indicated that there is no depth dependence of stress drops. Wu et al. (2018) analyzed four (4) induced earthquake sequences in Oklahoma, USA and did not observed apparent depth dependence.

The relationship with the depth dependence of the static stress drop, the corner frequency and the seismic moment are shown in Figures 4a, b, and c, respectively. As seen from the Figure 4a, the static stress drop values show scattered behavior and we can conclude that we did not find a clear depth dependence of the stress drop values. Similar behavior is also seen for depth dependence of the corner frequency (Fig. 4b). Even though there is no clear

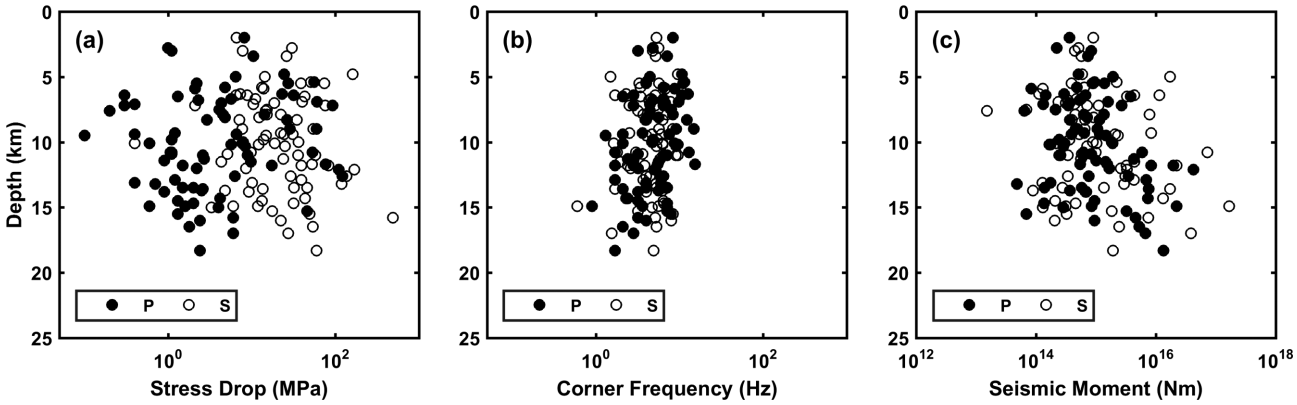


Fig. 4. Depth dependence of (a) stress drop, (b) corner frequency, and (c) seismic moment determined from P (black circles) and S (white circles) wave spectra.

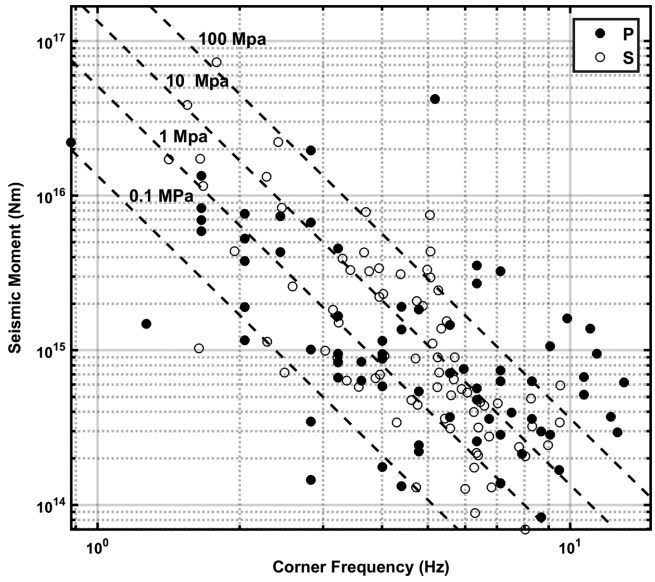


Fig. 5. Seismic moment-corner frequency relationship for the analyzed events. Lines of constant indicate Brune stress drop 0.1, 1, 10 and 100 MPa.

depth dependence but it seems that deeper events have lower corner frequency values. The depth dependence of the seismic moment is clearer than the stress drop and the corner frequency. Figure 4c shows that deeper events have larger seismic moment values.

Figure 5 shows seismic moment versus corner frequency for the analyzed events. Lines of constant Brune stress drop are 0.1, 1, 10 ve 100 MPa. It is noticed that most of events appear to scale self-similarly. However, a number of events have larger and smaller stress drop values. The high stress drops for these events can indicate high frictional strength and low strain-rate of the faults. Similarly, the low values of the stress drop can indicate a general weakness of the faults in the study area.

The magnitude saturation is an important problem for the accurate identification of the earthquake magnitude. It is known that moment magnitude is not saturated in different magnitude definitions (Hanks and Kanamori, 1979) and therefore important in seismic hazard calculations. Several authors have obtained relations between local magnitude (M_L) and M_W for different regions of the world (Uhrhammer et al., 1996). Therefore, it is important to find such an empirical relationships relating M_W. The relationship between the moment magnitudes calculated by P and S wave displacement spectrum and the local magnitude scale defined by KOERI has been shown in Figure 6. But, some scattering, especially in small magnitudes are observed in Figure 6. We can link the causes of this scattering to some negative effects which are seen in local magnitude calculation. M_L is calculated by using Wood-Anderson (WA) seismograph or displacement seismograms are simulated by Wood-Anderson seismograph transfer function. But, there is a confusion about the amplification of the Wood Anderson seismographs. Typical WA seismograph had an amplification of 2.800 which KOERI uses this value (D. Kalafat, personal communication). Uhrhammer and Collins (1990) and Uhrhammer et al. (1996) have indicated that the effective amplification of the typical WA seismograph is around 2.080 (Scordilis, 2006). On the other hand, natural period of the WA is 1.25 Hz. But dominant frequency is shifting higher frequencies than 1.25 Hz for smaller earthquakes. Also, if azimuthal distribution is neglecting or not good enough, rupture effects such as directivity also affected the wave amplitudes. Additionally, complexity of source processes of analyzed earthquakes and site effects could be effected on the wave amplitudes and therefore scattering. These effects are leading to systematic errors in M_L estimations and could be an explanation for scattering in small magnitudes in Figure 6.

The least squares method is one of the most frequently used methods in regression analysis. However, a least squares estimate for regression models are highly sensitive to outliers which is a case in magnitude scattering in this study. Therefore, we computed different type of regressions analysis compared to determine the

https://doi.org/10.1007/s12303-019-0039-2

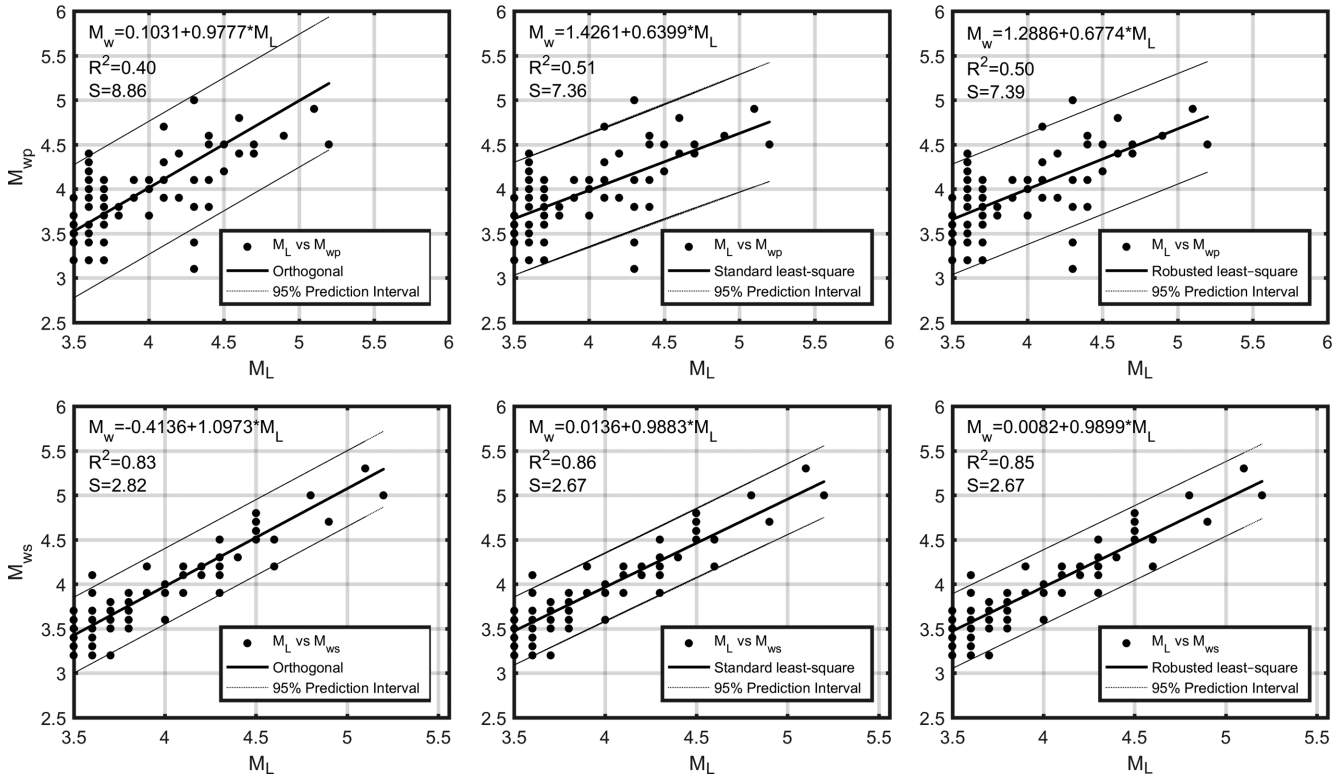


Fig. 6. Comparison of orthogonal, standard and robusted least square regression analysis for determining M_W-M_L relationship. M_{WP} indicates M_W magnitude obtained from P wave spectra and M_{WS} indicates M_W magnitude obtained from S wave spectra. R^2 indicates correlation coefficient.

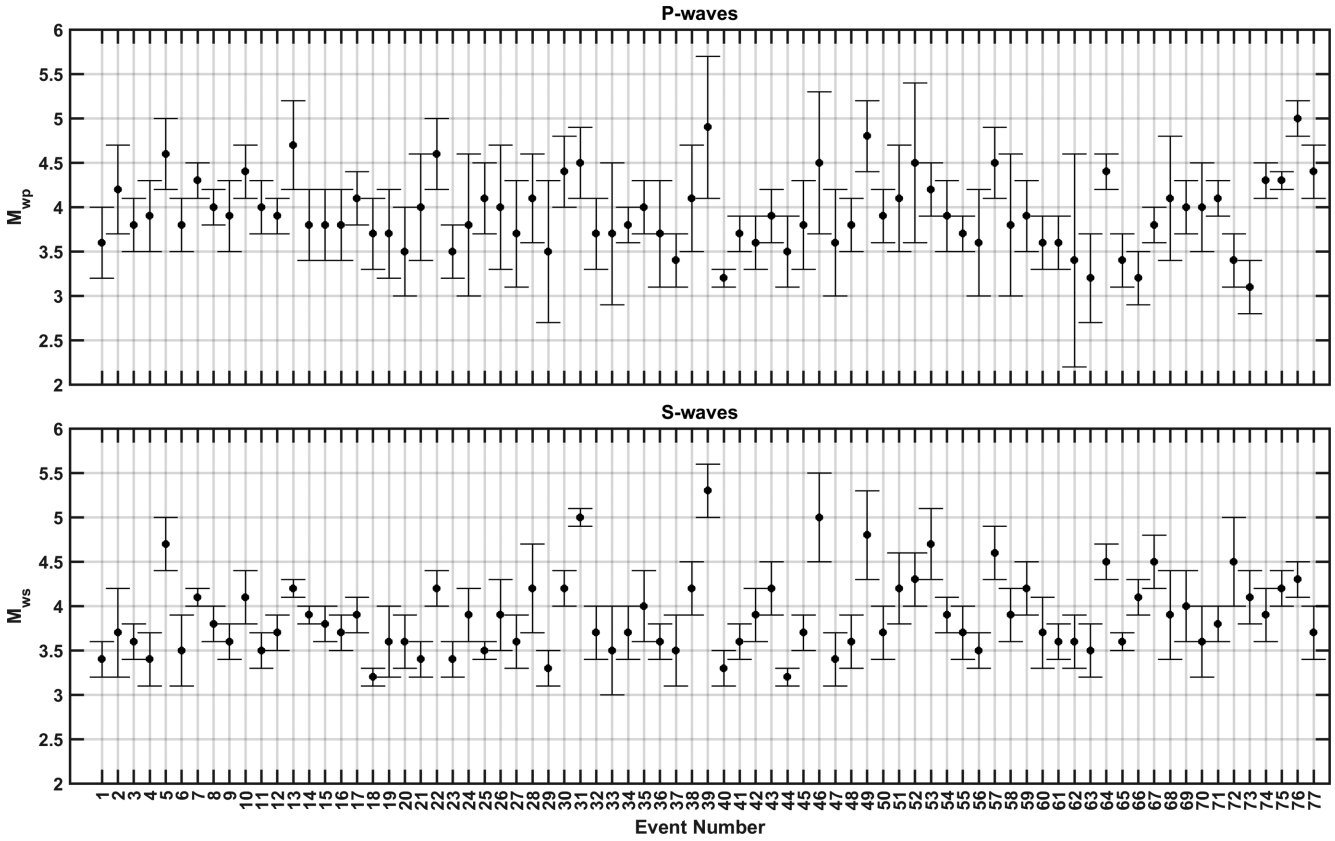


Fig. 7. Standard deviation values for all calculated $M_{W(P,S)}$.

best one to use. We tried to test standard least-squares (minimizing the square of the vertical offsets to the best-fit line), robusted least-squares (attempt to dampen the influence of outlying cases in order to provide a better fit to the majority of the data), and orthogonal regression (minimizing the square of the perpendicular offsets to the best-fit line). The R^2 values obtained by the standard least-square and the robusted least-square methods are very close to each other. However, we preferred the largest R^2 value has been obtained from standard least-squares regression analysis (Fig. 6) as the M_W-M_L relationship,

$$M_W = 1.4261(\pm 0.31) + 0.6399(\pm 0.08)M_L \text{ (for P wave)}, \quad (7)$$

$$M_W = 0.0136(\pm 0.21) + 0.9883(\pm 0.05)M_L \text{ (for S wave)}. \quad (8)$$

Standard deviation for M_W and $\Delta\sigma$ all events are also given in

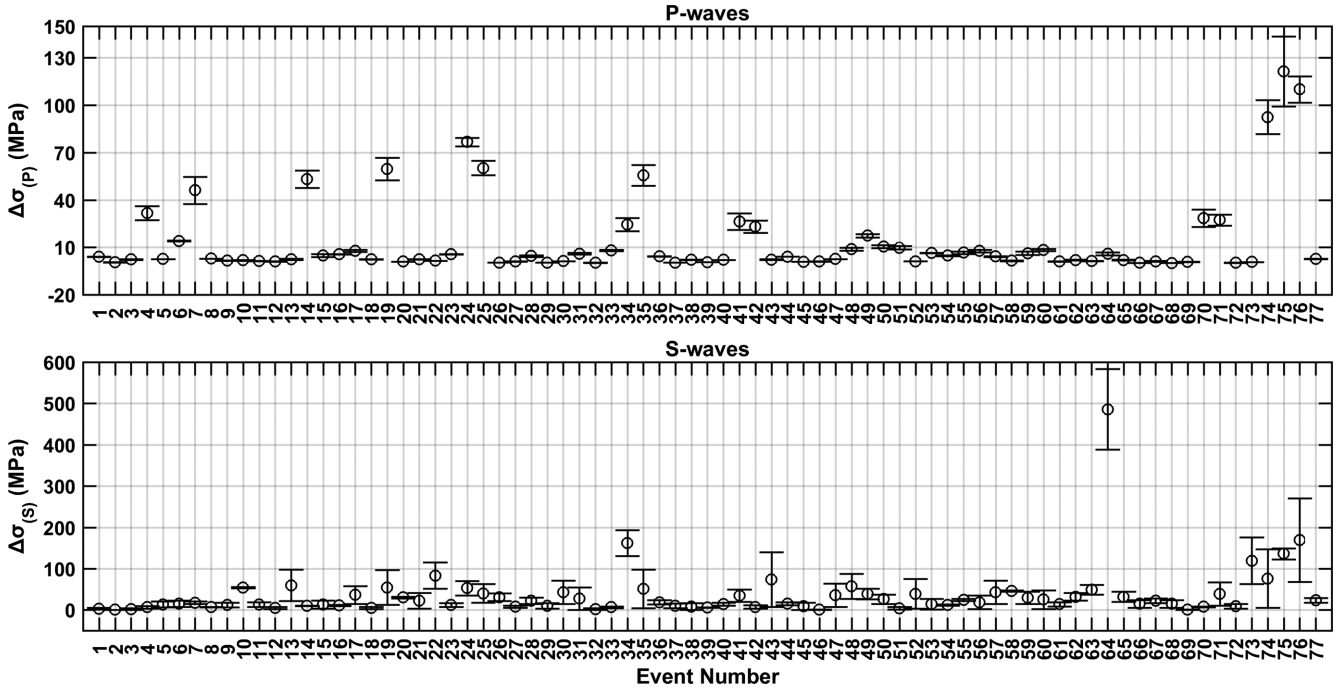


Fig. 8. Standard deviation values for all calculated stress drop ($\Delta\sigma_{(P,S)}$).

Table 3. Comparison of calculated M_w in this study and M_w values announced by other agencies for the same earthquake

Event Number	Earthquake	$M_{w(P)}$ (this study)	$M_{w(S)}$ (this study)	Mw
5	10072008_074953	4.6	4.7	4.5 (KOERI) 4.7 (INGV)
10	24012009_155838	4.4	4.1	4.3 (KOERI) 4.0 (ERD)
13	27042009_190306	4.7	4.2	3.8 (ERD) 4.3 (KOERI)
30	11072011_160912	4.4	4.2	4.5 (ERD)
31	25072011_175720	4.5	5.0	4.9 (ERD) 4.9 (GFZ) 5.0 (KOERI)
39	06072012_205425	4.9	5.3	4.9 (ERD) 4.9 (GFZ) 4.9 (AUTH) 5.1 (KOERI) 5.1 (NOA)
52	16122014_090213	4.5	4.3	4.1 (ERD)
73	22072017_221232	3.1	4.1	3.9 (ERD)
76	30112018_023635	5.0	4.3	4.0 (KOERI) 4.0 (ERD)

ERD: Earthquake Research Department, Ankara; KOERI: Kandilli Observatory and Earthquake Research Institute, İstanbul; GFZ: GeoForschunzg Zentrum, Germany; AUTH: Aristotle University of Thessaloniki, Greece; NOA; National Observatory of Athens, Greece; INGV: Istituto Nazionale Di Geofisica E Vulcanologia, Italy.

$M_{w(P)}$: Moment magnitude calculated from P wave spectra; $M_{w(S)}$: Moment magnitude calculated from S wave spectra.

https://doi.org/10.1007/s12303-019-0039-2

Figures 7 and 8, respectively.

Table 3 shows the moment magnitude calculated in this study and the moment magnitude determined by other seismological agencies. It is seen that the calculated moment magnitudes are mostly compatible (especially relationship obtained from S wave spectra) with the magnitudes calculated by different agencies.

Parolai et al. (2007) studied source parameters of the eastern Marmara Region. They studied 523 aftershocks ($0.5 < M_L < 5.9$) of the 1999 Kocaeli earthquake and determined that the stress drop values were changing between 0.002–40 MPa. Parolai et al. (2007) suggested that the seismic moment range between 1.05e14 and 2.41e14 Nm. Köseoğlu et al. (2014) analyzed 174 events ($2.5 < M_L < 5.5$) that occurred western part of Turkey including Marmara region. Köseoğlu et al. (2014) reported that the seismic moments are in range 1.28e14 to 1.66e14 Nm, stress drops on the fault are in range 0.17 to 6476 MPa and corner frequencies are 0.2 to 15 Hz, and the source sizes of the events are 0.0862 to 5.1042 km. This study covered whole Marmara region and our results are comparable with the study of Parolai et al. (2007) and Köseoğlu et al. (2014).

5. CONCLUSIONS

In this study, we tried to understand the relationships between the source parameters of 77 earthquakes with local magnitude ranging from 3.5 to 5.2 occurring in the Marmara region. The dynamic source parameters have been derived from P and S wave spectra. Distance correction attenuation parameters for the low-frequency amplitude and for the corner frequency have been obtained, and the seismic moment, M_0, moment magnitude, M_W, source radius, r, and stress drop, $\Delta\sigma$ *have* been calculated.

It is found that f_c is dependent on seismic moment, f_c decreases with the increase of the seismic moment as expected. $f_c(P)/f_c(S)$ ratio is found 1.3. The obtaining seismic moment M_0 and source radius r, are varying between 4.83×10^{13} and 1.68×10^{17} Nm and 146–4486 m, respectively. The values of stress drop $\Delta\sigma$ vary between 0.1 and 136 MPa with a mean value of 9.8 MPa (98 bars). The high stress drops for these events indicate high frictional strength and low strain rate of the faults as well as the low value of the stress drop indicate the general weakness of the faults in the study area. There is no clear dependence between the seismic moment and the static stress drop. However, there is a turning point around magnitude 4, the stress drop values for the events that magnitudes smaller than 4 ($M < 4$) are increasing with the magnitude. Also, a clear depth dependence of the stress drop values has not been observed. Similarly, depth dependence of corner frequency has not been observed. The depth dependence of the seismic moment is seen more clearly. Our results indicated that the deeper events have larger seismic moment values in the study area. In spite of scattering in small events, a linear relationship between local magnitude (M_L) and moment magnitude (M_W) could be obtained as $M_W = 1.4261(\pm 0.31) + 0.6399(\pm 0.08)M_L$ from P waves spectra and $M_W = 0.0136(\pm 0.21) + 0.9883(\pm 0.05)M_L$ from S wave spectra and calculated M_W values are consistent with waveform inversion (centroid moment tensor – CMT) results. These relationships may be useful for seismic hazard studies in the study area.

ACKNOWLEDGMENTS

The authors would like to thanks two anonymous reviewers for their helpful comments that improved the manuscripts. The authors would like to thank the KOERI-NEMC staff to provide waveform data.

REFERENCES

Abercrombie, R.E., 1995, Earthquake source scaling relationships from −1 to 5 ML using seismograms recorded at 2.5-km depth. Journal of Geophysical Research: Solid Earth, 100, 24015–24036.

Allen, T.I., Gibson, G., Brown, A., and Cull, J.P., 2004, Depth variation of seismic source scaling relations: implications for earthquake hazard in southeastern Australia. Tectonophysics, 390, 5–24.

Allmann, B.P. and Shearer, P.M., 2007, Spatial and temporal stress drop variations in small earthquakes near Parkfield, California. Spatial and temporal stress drop variations in small earthquakes near Parkfield, California. Journal of Geophysical Research, 112, B04305. https://doi.org/10.1029/2006JB004395

Allmann, B.P. and Shearer, P.M., 2009, Global variations of stress drop for moderate to large earthquakes. Journal of Geophysical Research: Solid Earth, 114, B01310. https://doi.org/10.1029/2008JB005821

Ambraseys, N.N., 1970, Some characteristic features of the Anatolian fault zone. Tectonophysics, 9, 143–165.

Armijo, R., Meyer, B., Hubert, A., and Barka, A., 1999, Westward propagation of the North Anatolian fault into the northern Aegean: timing and kinematics. Geology, 27, 267–270.

Armijo, R., Meyer, B., Navarro, S., King, G., and Barka, A., 2002, Asymmetric slip partitioning in the Sea of Marmara pull-apart: a clue to propagation processes of the North Anatolian fault? Terra Nova, 14, 80–86.

Armijo, R., Meyer, B., Barka, A., Chabalier, J.B., Hubert-Ferrari, A., and Çakir, Z., 2000, The fault breaks of the 1999 earthquakes in Turkey and the tectonic evolution of the Sea of Marmara: a summary. In: Barka, A., Kozacı, Ö., Akyüz, S., and Altunel, E. (eds.), The 1999 Izmit and Düzce Earthquakes: Preliminary Results. İstanbul Technical University Press, İstanbul, p. 55–62.

Armijo, R., Pondard, N., Meyer, B., Uçarkus, G., de Lépinay, B.M., Malavieille, J., Dominguez, S., Gustcher, M.A., Schmidt, S., Beck, C., and Cagatay, N., 2005, Submarine fault scarps in the Sea of Marmara pull-apart (North Anatolian Fault): implications for seismic hazard in Istanbul. Geochemistry, Geophysics, Geosystems, 6, https://doi.org/10.1029/2004GC000896

Asano, K., Iwata, T., and Irikura, K., 2003, Source characteristics of shallow intraslab earthquakes derived from strong-motion simulations. Earth, Planets and Space, 55, e5–e8.

Ataeva, G., Shapira, A., and Hofstetter, A., 2015, Determination of source parameters for local and regional earthquakes in Israel. Journal of Seismology, 19, 389–401.

Barka, A., 1992, The north Anatolian fault zone. Annales Tectonicae, 6, 164–195 (Suppl).

Barka, A., 1996, Slip distribution along the North Anatolian fault associated with the large earthquakes of the period 1939 to 1967. Bulletin of the Seismological Society of America, 86, 1238–1254.

Barka, A., 1999, The 17 August 1999 Izmit earthquake. Science, 285, 1858–1859.

Barka, A. and Kadinsky-Cade, K., 1988, Strike-slip fault geometry in Turkey and its influence on earthquake activity. Tectonics, 7, 663–684.

Bayrakci, G., Laigle, M., Bécel, A., Hirn, A., Taymaz, T., Yolsal-Çevikbilen, S., and Team, S., 2013, 3-D sediment-basement tomography of the Northern Marmara trough by a dense OBS network at the nodes of a grid of controlled source profiles along the North Anatolian fault. Geophysical Journal International, 194, 1335–1357.

Bilek, S.L. and Lay, T., 1998, Variation of interplate fault zone properties with depth in the Japan subduction zone. Science, 281, 1175–1178.

Brune, J.N., 1970, Tectonic stress and the spectra of seismic shear waves from earthquakes. Journal of Geophysical Research, 75, 4997–5009.

Brune, J.N., 1971, Correction [to "Tectonic stress and the spectra, of seismic shear waves from earthquakes"]. Journal of Geophysical Research, 76, 5002. https://doi.org/10.1029/JB076i020p05002

Boatwright, J., 1980, A spectral theory for circular seismic sources; simple estimates of source dimension, dynamic stress drop, and radiated seismic energy. Bulletin of the Seismological Society of America, 70, 1–27.

Boatwright, J., Fletcher, J.B., and Fumal, T.E., 1991, A general inversion scheme for source, site, and propagation characteristics using multiply recorded sets of moderate-sized earthquakes. Bulletin of the Seismological Society of America, 81, 1754–1782.

Bulut, F., Bohnhoff, M., Ellsworth, W.L., Aktar, M., and Dresen, G., 2009, Microseismicity at the North Anatolian fault in the Sea of Marmara offshore Istanbul, NW Turkey. Journal of Geophysical Research: Solid Earth, 114. https://doi.org/10.1029/2008JB006244

Candela, T., Renard, F., Bouchon, M., Schmittbuhl, J., and Brodsky, E.E., 2011, Stress drop during earthquakes: effect of fault roughness scaling. Bulletin of the Seismological Society of America, 101, 2369–2387.

Chouet, B., Aki, K., and Tsujiura, M., 1978, Regional variation of the scaling law of earthquake source spectra. Bulletin of the Seismological Society of America, 68, 49–79.

Demirbağ, E., Rangin, C., Le Pichon, X., and Şengör, A.C., 2003, Investigation of the tectonics of the Main Marmara Fault by means of deep-towed seismic data. Tectonophysics, 361, 1–19.

Fichtner, A., Saygin, E., Taymaz, T., Cupillard, P., Capdeville, Y., and Trampert, J., 2013a, The deep structure of the North Anatolian fault zone. Earth and Planetary Science Letters, 373, 109–117.

Fichtner, A., Trampert, J., Cupillard, P., Saygin, E., Taymaz, T., Capdeville, Y., and Villasenor, A., 2013b, Multiscale full waveform inversion. Geophysical Journal International, 194, 534–556.

Fletcher, J.B., 1980, Spectra from high-dynamic range digital recordings of Oroville, California aftershocks and their source parameters. Bulletin of the Seismological Society of America, 70, 735–755.

Franceschina, G., Kravanja, S., and Bressan, G., 2006, Source parameters and scaling relationships in the Friuli-Venezia Giulia (Northeastern Italy) region. Physics of the Earth and Planetary Interiors, 154, 148–167.

Frankel, A., 1981, Source parameters and scaling relationships of small earthquakes in the northeastern Caribbean. Bulletin of the Seismological Society of America, 71, 1173–1190.

Garcia, J.G., Romacho, M.D., and Jiménez, A., 2004, Determination of near-surface attenuation, with κ parameter, to obtain the seismic moment, stress drop, source dimension and seismic energy for microearthquakes in the Granada Basin (Southern Spain). Physics of the Earth and Planetary Interiors, 141, 9–26.

Gök, R., Hutchings, L., Mayeda, K., and Kalafat, D., 2009, Source parameters for 1999 North Anatolian fault zone aftershocks. Pure and Applied Geophysics, 166, 547–566.

Hanks, T.C. and Wyss, M., 1972, The use of body-wave spectra in the determination of seismic-source parameters. Bulletin of the Seismological Society of America, 62, 561–589.

Hanks, T.C. and Kanamori, H., 1979, A moment magnitude scale. Journal of Geophysical Research: Solid Earth, 84, 2348–2350.

Hardebeck, J.L. and Hauksson, E., 1997, Static stress drop in the 1994 Northridge, California, aftershock sequence. Bulletin of the Seismological Society of America, 87, 1495–1501.

Hardebeck, J.L. and Aron, A., 2009, Earthquake stress drops and inferred fault strength on the Hayward fault, east San Francisco Bay, California. Bulletin of the Seismological Society of America, 99, 1801–1814.

Haskell, N.A., 1964, Total energy and energy spectral density of elastic wave radiation from propagating faults. Bulletin of the Seismological Society of America, 54, 1811–1841.

Havskov, J. and Ottemöller, L., 2010, Location. In: Havskov, J. and Ottemöller, L. (eds.), Routine Data Processing in Earthquake Seismology. Springer, Dordrecht, p. 101–149.

Horasan, G., Ayşe, K.Ö., Aysun, B.G., and Niyazi, T., 1998, S-wave attenuation in the Marmara Region, northwestern Turkey. Geophysical Research Letters, 25, 2733–2736.

Huang, M.H., Fielding, E.J., Dickinson, H., Sun, J., Gonzalez-Ortega, J.A., Freed, A.M., and Bürgmann, R., 2017, Fault geometry inversion and slip distribution of the 2010 Mw 7.2 El Mayor-Cucapah earthquake from geodetic data. Journal of Geophysical Research: Solid Earth, 122, 607–621.

Hubert-Ferrari, A., Barka, A., Jacques, E., Nalbant, S.S., Meyer, B., Armijo, R., Tapponnier, P., and King, G.C., 2000, Seismic hazard in the Marmara Sea region following the 17 August 1999 Izmit earthquake. Nature, 404, 269.

Imren, C., Le Pichon, X., Rangin, C., Demirbağ, E., Ecevitoğlu, B., and Görür, N., 2001, The North Anatolian Fault within the Sea of Marmara: a new interpretation based on multi-channel seismic and multi-beam bathymetry data. Earth and Planetary Science Letters, 186, 143–158.

Irmak, T.S., 2000, The source-rupture processes of recent large Turkey

earthquakes. Individual studies by participants to the International Institute of Seismology and Earthquake Engineering, 36, 131–143.

Irmak, T.S., Grosser, H., Özer, M.F., Woith, H., and Barış, S., 2007, The 24 October 2006 Gemlik Earthquake (M = 5.2). Geophysics Research Abstract, 9, 10212.

Jin, A., Moya, C.A., and Ando, M., 2000, Simultaneous determination of site responses and source parameters of small earthquakes along the Atotsugawa fault zone, central Japan. Bulletin of the Seismological Society of America, 90, 1430–1445.

Jones, L.E. and Helmberger, D.V., 1996, Seismicity and stress-drop in the Eastern Transverse Ranges, southern California. Geophysical Research Letters, 23, 233–236.

Kalafat, D., 1987, Bati Turkiye'de Kabuk Yapisi ve ust manto arastirilmasi. Deprem Arastirma Bulteni, 59, 43–64. (in Turkish)

Karabulut, H., Özalaybey, S., Taymaz, T., Aktar, M., Selvi, O., and Kocaoğlu, A., 2003, A tomographic image of the shallow crustal structure in the Eastern Marmara. Geophysical Research Letters, 30. https://doi.org/10.1029/2003GL018074

Keilis-Borok, V.I., 1960, Investigation of the mechanism of earthquakes. Soviet Research Geophysics (English translation), 4, 29.

Kinscher, J., Krüger, F., Woith, H., Lühr, B.G., Hintersberger, E., Irmak, T.S., and Baris, S., 2013, Seismotectonics of the Armutlu peninsula (Marmara Sea, NW Turkey) from geological field observation and regional moment tensor inversion. Tectonophysics, 608, 980–995.

Köseoğlu, A., Özel, N.M., Barış, Ş., Üçer, S.B., and Ottemöller, L., 2014, Spectral determination of source parameters in the Marmara Region. Journal of Seismology, 18, 651–669.

Kumar, A., Mitra, S., and Suresh, G., 2015, Seismotectonics of the eastern Himalayan and Indo-Burman plate boundary systems. Tectonics, 34, 2279–2295.

Kumar, A., Kumar, A., Mittal, H., Kumar, A., and Bhardwaj, R., 2012, Software to estimate earthquake spectral and source parameters. International Journal of Geosciences, 3, 1142–1149.

Kumar, A., Kumar, A., Gupta, S.C., Jindal, A.K., and Ghangas, V., 2014, Seismicity and source parameters of local earthquakes in Bilaspur region of Himachal Lesser Himalaya. Arabian Journal of Geosciences, 7, 2257–2267.

Kurtuluş, C. and Canbay, M.M., 2007, Tracing the middle strand of the North Anatolian Fault Zone through the southern Sea of Marmara based on seismic reflection studies. Geo-Marine Letters, 27, 27–40.

Le Pichon, X., Chamot-Rooke, N., Rangin, C., and Şengör, A.M.C., 2003, The North Anatolian fault in the sea of Marmara. Journal of Geophysical Research: Solid Earth, 108. https://doi.org/10.1029/2002JB001862

Le Pichon, X., Şengör, A.M.C., Demirbağ, E., Rangin, C., Imren, C., Armijo, R., Görür, N., Çağatay, N., Mercier de Lepinay, B., Meyer, B., Saatçılar, R., and Tok, B., 2001, The active Main Marmara Fault. Earth and Planetary Science Letters, 192, 595–616.

McClusky, S., Balassanian, S., Barka, A., Demir, C., Ergintav, S., Georgiev, I., Gurkan, O., Hamburger, M., Hurst, K., Kahle, H., and Kastens, K., 2000, Global positioning system constraints on plate kinematics and dynamics in the eastern Mediterranean and Caucasus. Journal of Geophysical Research: Solid Earth, 105, 5695–5719.

Nalbant, S.S., Hubert, A., and King, G.C., 1998, Stress coupling between earthquakes in northwest Turkey and the north Aegean Sea. Journal of Geophysical Research: Solid Earth, 103, 24469–24486.

Okay, A.İ., Kaşlılar-Özcan, A., Imren, C., Boztepe-Güney, A., Demirbağ, E., and Kuşçu, I., 2000, Active faults and evolving strike-slip basins in the Marmara Sea, northwest Turkey: a multichannel seismic reflection study. Tectonophysics, 321, 189–218.

Oth, A., Bindi, D., Parolai, S., and Di Giacomo, D., 2010, Earthquake scaling characteristics and the scale-(in)dependence of seismic energy-to-moment ratio: insights from KiK-net data in Japan. Geophysical Research Letters, 37. https://doi.org/10.1029/2010GL044572

Oye, V., Bungum, H., and Roth, M., 2005, Source parameters and scaling relations for mining-related seismicity within the Pyhasalmi ore mine, Finland. Bulletin of the Seismological Society of America, 95, 1011–1026.

Parolai, S., Bindi, D., Durukal, E., Grosser, H., and Milkereit, C., 2007, Source parameters and seismic moment-magnitude scaling for Northwestern Turkey. Bulletin of the Seismological Society of America, 97, 655–660.

Prieto, G.A., Shearer, P.M., Vernon, F.L., and Kilb, D., 2004, Earthquake source scaling and self-similarity estimation from stacking P and S spectra. Journal of Geophysical Research: Solid Earth, 109. https://doi.org/10.1029/2004JB003084

Reilinger, R.E., Ergintav, S., Bürgmann, R., McClusky, S., Lenk, O., Barka, A., Gurkan, O., Hearn, L., Feigl, K.L., Cakmak, R., and Aktug, B., 2000, Coseismic and postseismic fault slip for the 17 August 1999, M = 7.5, Izmit, Turkey Earthquake. Science, 289, 1519–1524.

Sato, T., Kasahara, J., Taymaz, T., Ito, M., Kamimura, A., Hayakawa, T., and Tan, O., 2004, A study of microearthquake seismicity and focal mechanisms within the Sea of Marmara (NW Turkey) using ocean bottom seismometers (OBSs). Tectonophysics, 391, 303–314. https://doi.org/10.1016/j.tecto.2004.07.018

Scordilis, E.M., 2006, Empirical global relations converting M_S and m_b to moment magnitude. Journal of seismology, 10, 225–236.

Sivaram, K., Kumar, D., Teotia, S.S., Rai, S.S., and Prakasam, K.S., 2013, Source parameters and scaling relations for small earthquakes in Kumaon Himalaya, India. Journal of Seismology, 17, 579–592.

Smith, A.D., Taymaz, T., Oktay, F., Yuce, H., Alpar, B., Basaran, H., Jackson, J.A., Kara, S., and Simsek, M., 1995, High-resolution seismic profiling in the Sea of Marmara (northwest Turkey): Late Quaternary sedimentation and sea-level changes. Geological Society of America Bulletin, 107, 923–936.

Stein, R.S., Barka, A., and Dieterich, J.H., 1997, Progressive failure on the North Anatolian fault since 1939 by earthquake stress triggering. Geophysical Journal International, 128, 594–604.

Süle, B. and Wéber, Z., 2013, Earthquake source parameters and scaling relationships in Hungary (central Pannonian basin). Journal of Seismology, 17, 507–521.

Taymaz, T., Jackson, J., and McKenzie, D., 1991, Active tectonics of the north and central Aegean Sea. Geophysical Journal International, 106, 433–490.

Toksöz, M.N., Shakal, A.F., and Michael, A.J., 1979, Space-time migration of earthquakes along the North Anatolian fault zone and seismic gaps. Pure and Applied Geophysics, 117, 1258–1270.

Tunc, B., Caka, D., Irmak, T.S., Woith, H., Tunc, S., Baris, S., Ozer, M.F., Lühr, B.G., Günther, E., Grosser, H., and Zschau, J., 2011, The Armutlu Network: an investigation into the seismotectonic setting of Armutlu-

Yalova-Gemlik and the surrounding regions. Annals of Geophysics, 54, 35–45. https://doi.org/10.4401/ag-4877

Tusa, G. and Gresta, S., 2008, Frequency-dependent attenuation of P waves and estimation of earthquake source parameters in southeastern Sicily, Italy. Bulletin of the Seismological Society of America, 98, 2772–2794.

Uhrhammer, R.A. and Collins, E.R., 1990, Synthesis of Wood-Anderson seismograms from broadband digital records. Bulletin of the Seismological Society of America, 80, 702–716.

Uhrhammer, R.A., Loper, S.J., and Romanowicz, B., 1996, Determination of local magnitude using BDSN broadband records. Bulletin of the Seismological Society of America, 86, 1314–1330.

Wu, Q. and Chapman, M., 2017, Stress-drop estimates and source scaling of the 2011 Mineral, Virginia, mainshock and aftershocks. Bulletin of the Seismological Society of America, 107, 2703–2720.

Wu, Q., Chapman, M., and Chen, X., 2018, Stress-drop variations of induced earthquakes in Oklahoma. Bulletin of the Seismological Society of America, 108, 1107–1123.

Zobin, V.M. and Havskov, J., 1995, Source spectral properties of small earthquakes in the northern North Sea. Tectonophysics, 248, 207–218.

Publisher's Note Springer Nature remains neutral with regard to jurisdictional claims in published maps and institutional affiliations.

https://doi.org/10.1007/s12303-019-0039-2